Soil Dynamics and Earthquake Engineering 139 (2020) 106416

Contents lists available at ScienceDirect

Soil Dynamics and Earthquake Engineering

journal homepage: http://www.elsevier.com/locate/soildyn

A full experimental and numerical modelling of the practicability of thin foam barrier as vibration reduction measure

M. Naghizadehrokni [a,*], M. Ziegler [a], J. Sprengel [b]

[a] RWTH Aachen University, Department of Civil Engineering, Chair of Geotechnical Engineering, Aachen, Germany
[b] Vössing Engineer, Former GiB RWTH Aachen University, Germany

A B S T R A C T

This paper presents the performance of geofoam-filled trenches in mitigating of ground vibration transmissions by the means of a full experimental study. The results are interpreted in the frequency domain. Fully automated 2*D* and 3*D* numerical models are applied to evaluate the screening effectiveness of geofoam-filled trenches in the active and passive schemes. Experimental results are in good agreement with the prediction of numerical modelling. The validated model is used to investigate the influence of geometrical and dimensional features on the trench. In addition, three different systems including single, double and triangle wall obstacles are selected for analysis, and the results are compared for various situations. The parametric study is based on complete automation of the model through coupling finite element analysis software (Plaxis) and Python programming language to control input, change the parameters, as well as to produce output and calculate the efficiency of the barrier. The results show that the depth and the width of approximately $1\lambda_r$ and $0.2\lambda_r$, respectively are enough to reach the acceptable amount of efficiency for the active isolation for all three systems. For the passive scheme, the role of depth can be ignored for the single and double wall barriers, while depth plays a significant role for the triangle wall system.

1. Introduction

In metropolitan cities, man-made ground vibrations generated by external dynamic sources including traffic, blasting, machine foundations and other constructional activities have recently become a major concern for the nearby structures and inhabitants. Most of the transmitted vibration energy is propagated by Rayleigh waves close to the soil surface. The rest of the energy is transmitted by the body waves [1]. Near-surface vibration can be a major problem for the surrounding buildings and their inhabitants. Therefore, implementing a wave barrier in the transmission path is a suitable solution as it allows scattering the ground-borne vibrations [2]. The barrier intercepts the dispatched waves through a complex mode of wave interactions including, reflection, refraction, diffraction and wave interference. Vibration screening is classified into two categories including the active scheme, in which the obstacle is installed near the source of vibration, and the passive scheme, in which the trench is constructed far away from the vibration source. On the other hand, the applicability of the wave barrier is classified in terms of open or in-filled trenches [3].

Several studies including both field tests [4,5] and numerical modelling [6–8] have been carried out in order to evaluate the efficiency of the wave barrier in wave attenuation. Woods [9] was one of the first to perform a full experimental test for evaluating the efficiency of open trenches. He suggested that a wave barrier should reach at least 75% mitigation in screening of incoming waves to be deemed as efficacious. In practice, however, open trenches are not applicable in many cases for a longer time due to difficulties in construction and stability problems. In such cases, in-filled trench obstacles are generally used.

A series of field tests are conducted by Ref. [10,11] for finding the screening effectiveness of open and geofoam-filled obstacles and found that the performance of geofoam-filled trench reached 68 and 67%, respectively. Multiple rows of geofoam-filled barriers are employed for assessing the applicability of trench in frequency domain [12]. They proved that increasing trench depth, to more than one wavelength has only negligible affect on screening performance in the passive scheme. Celebi et al. [13] described the results of experimental studies to compute the screening efficiency of open, stiff and soft barriers in the case of active and passive schemes. The observations illustrated that the passive isolation is more effective than the active isolation and softer back-fill material can be more effective in attenuating the incoming waves in comparison with the stiff materials. In addition, a centrifuge parametric investigation is accomplished by Ref. [14] to examine the effect of dimensional and geometrical factors on the geofoam-filled trench in the mitigation of incident waves. The results of the study showed that the screening performance is dependent on the trench depth.

* Corresponding author.
E-mail address: naghizadehrokni@geotechnik.rwth-aachen.de (M. Naghizadehrokni).

https://doi.org/10.1016/j.soildyn.2020.106416
Received 4 May 2020; Received in revised form 11 August 2020; Accepted 6 September 2020
0267-7261/© 2020 Elsevier Ltd. All rights reserved.

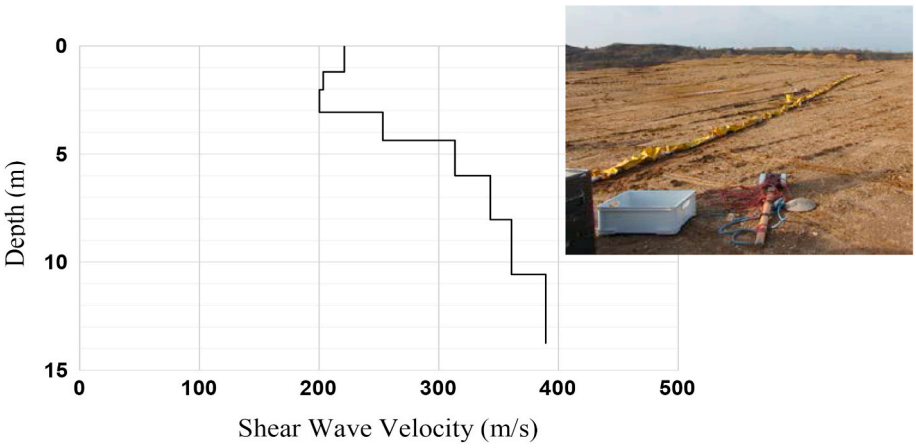

Fig. 1. Shear wave velocity profile of the site.

In addition, numerical techniques including the finite element method (FEM) and the boundary element method (BEM) can be used as powerful tools to study the screening performance of wave barriers. Beskos et al. [15–17] developed a BEM model to determine the screening capability of open and concrete-filled trenches in homogeneous and layered soil. Ahmad and Al-Hussaini [18] conducted an extensive parametric study to analyse the influence of different geometrical and material parameters on the screening efficiency of rectangular open and concrete-filled obstacles. Finally, they developed a simple model for vibration isolation in active and passive schemes. Haupt [19,20] also used numerical modelling for assessing the vibration isolation performance. He suggested that the trench depth should be at least 80% of the R-wavelength (λ_r) to reach a successful attenuation. A FEM is developed to evaluate the efficiency of water and geofoam-filled trenches [21,22]. They observed that the depth of the barrier is the governing factor in increasing the efficiency of the barrier and width and length of the trench do not play a significant role in screening performance. Majumder et al. [23–25] performed some numerical modelling in order to evaluate the efficiency of the geofoam-filled trench. They suggested the normalized depth equal to 1 as the optimum value for reaching the highest value of the efficiency. In addition, they stated that increasing the frequency of the vibration source results in increasing the efficiency of the trench. Qiu et al. [26] established a 2*D* numerical model for a comparative study on vibration isolation effectiveness and developed a model for optimizing various dimensions of the barrier. Concerning different configurations of the barriers, Saikia [27] and Schevenels et al. [28] considered double wall barriers, Esmaeili et al. [29,30] evaluated the effectiveness of V-shaped and step-shaped trenches and Alzawi et al. [31] conducted a comprehensive study for computing the performance of geofoam-filled barriers in the form of box-walls, single and double wall systems.

Studying the literature revealed that a full experimental test and a parametric investigation to examine the efficiency of various configurations of geofoam-filled trenches are required. This paper deals with filling this gap through a field test and a comprehensive parametric study. The results of the field tests for evaluating the efficiency of geofoam-filled barrier in mitigating the incident waves in the frequency domain are presented in section 2. 2*D* and a 3*D* finite element models are developed and the validity of the models are compared with the results of the full experimental test as shown in section 3.1. Subsequently, different configurations including single, double and triangle wall systems are selected for evaluating the performance of vibration screening in the active and passive schemes in sections 4 and 5, respectively. Various parameters including geometrical parameters and dimensional factors that govern the screening performance are considered for more assessing.

2. Field test

2.1. Site investigation

A full experimental test has conducted [32] to analyse the efficiency of the geofoam-filled trench in screening dispatched waves. The subsoil properties and the location of the field test are one the most important features. The main criteria for selecting the site location are considered as homogeneity of the soil, easy accessibility to the test site and possibility of the implementation of the trench. For these purposes, the location of the test site has selected in a gravel pit based on a flat area with dimensions of approximately $40m \times 60m$, located in Geilenkirchen, a town in North Rhine-Westphalia.

The soil analysis consisted of soil classification and has done on some samples from different depths. The result of laboratory test of the soil demonstrated that the subsoil is a mixture of sand and gravel up to a depth of at least 15*m*. According to DIN 18196, the soil is classified as intermittent graded sand. The medium soil density was determined to ($\rho = 2g/cm^3$).

The Multichannel Analysis of Surface Waves method (MASW) was used to determine the dynamic elastic material parameters, which are key factors for describing the soil dynamic behaviour of the subsoil. MASW is a geophysical procedure for determining the depth-dependent profile of the propagated shear wave velocity. The data were recorded over a total of 48 geophones, which were laid out at a distance of 1*m*, and registered by a seismograph. Fig. 1 shows the geophones in the field test and the determined profile of the propagation velocity of the shear wave over the depth as an average value over the entire measuring section (see Fig. 2.

2.2. Field test method and equipment

A shaker from Baudynamik Heiland & Mistler GmbH was used (see Fig. 2*A*), which allows to produce a harmonic excitation of the ground. The shaker [42] was founded on four steel plates and the overall dimensions of the shaker were 72*72*cm*. The servo-hydraulic shaker simulated the requested objects, in this case, harmonic load in the frequency range of theoretically 0.01 to 110*Hz* with a maximum dynamic force amplitude of 15*kN*. The force amplitude generated in the field test was constantly 5*kN* in the frequency range from 10*Hz* to 110*Hz*, but only the range from 20*Hz* to 80*Hz* was used for trench efficiency evaluation [32].

The measurement of the vertical soil particle velocity had been done two times, before installation the trench and one after implementation of the geofoam-filled barrier. The measuring chain in the field test consisted of the vibration sensors including geophone and accelerometer shown in Fig. 2*B*, which transmitted their data to a measuring computer.

Fig. 2. Vibration source: (A) Shaker structural dynamics Heiland & Mistler GmbH, (B) Vibration sensor.

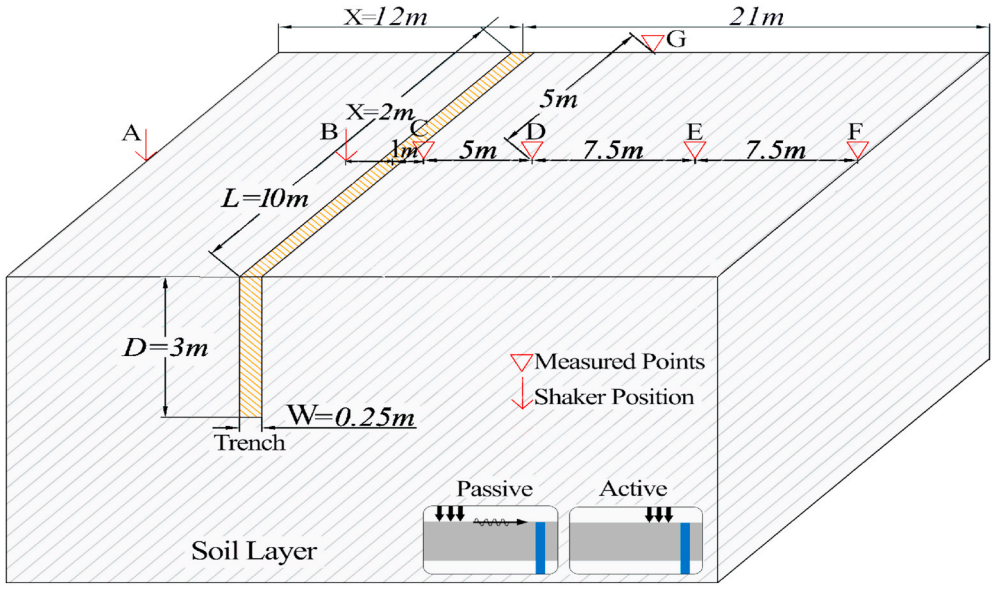

Fig. 3. Measuring arrangement.

The transferred data were analysed by MESSI, a program developed by the Department of Structural Mechanics at RWTH Aachen University for signal acquisition and processing. Some distinct points were selected for installing vibration sensors with different distances from the source of vibration and the obstacle. Fig. 3 illustrates the selected measuring arrangement including the positioning of the vibration source, the geofoam-filled barrier and the vibration sensors, respectively.

The shaker was located at two different distances from the trench. To investigate the effectiveness of the obstacle for both situations, the vibration source had appropriately positioned relative to the barrier. Due to the limited number of available vibration sensors, seven measuring points were selected per measurement series, with measuring points A and B located directly on the shaker for the passive and active isolation, respectively.

An approximate propagation velocity of the R-wavelength at the surface of $v_r = 200m/s$ and a minimum and maximum examined

Fig. 4. Wheel trench device and injection of geofoam.

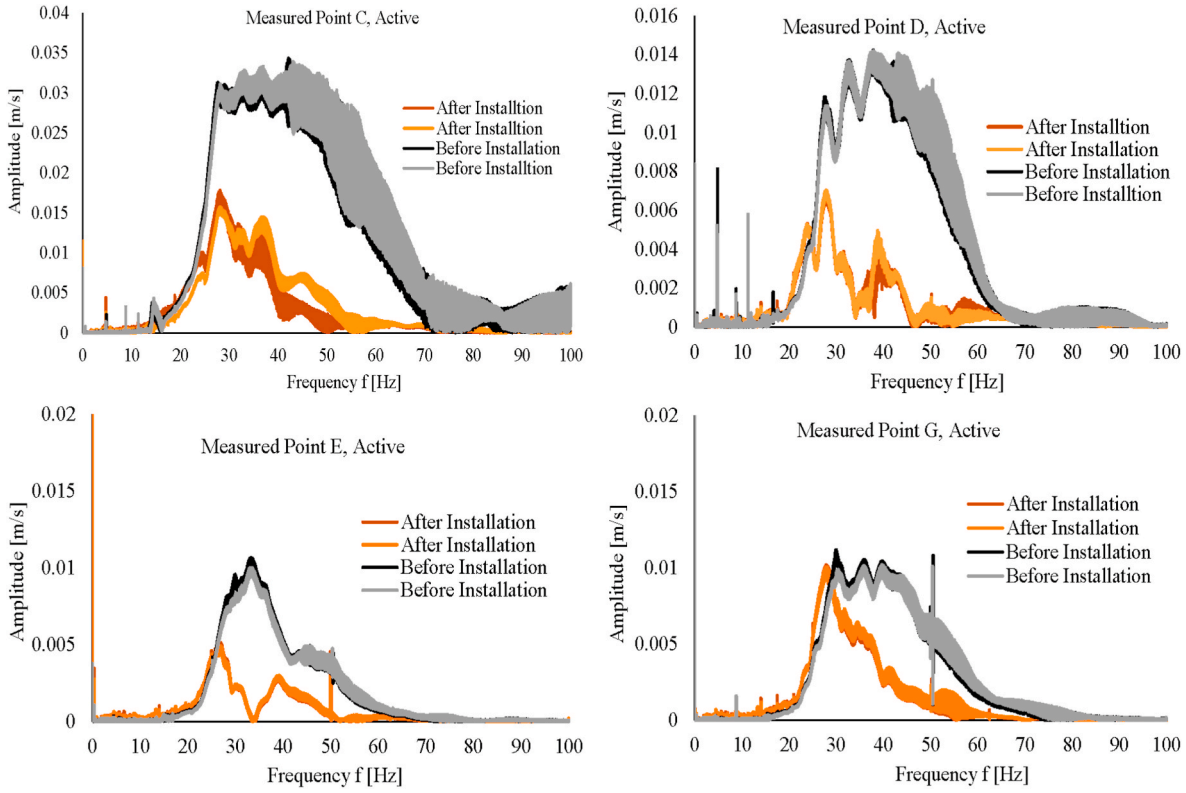

Fig. 5. Representation in the frequency domain: Measuring points C, D, E, G (Active Isolation).

frequency of 20 and 100*Hz* leads to a wavelength of $\lambda_r = 10$ and 2*m*. Therefore, the position of vibration source was chosen 2*m* for the active isolation and 12*m* for the passive isolation, respectively. Excavating a trench for mitigating of incident waves was the next step after measuring the vertical soil particle velocity in the absence of the barrier. Most of previous studies [8,15,33] stated that a normalized depth of $0.8\lambda_r$ is enough to reach acceptable value of the efficiency. Therefore, an attempt was made to reach this depth during the experimental test. A wheel trencher device was used for digging the trench with the dimensions of 3.2*m* depth, 20*cm* width and 10*m* length. However, the excavating process to reach this depth failed because of facing hard soil in some sections. Therefore, the excavated depth of the barrier was between $2.8 - 3.2m$ and the average depth of 3*m* was considered for whole trench. The low stability of the trench due to the kind of soil resulted in a very short stability of the barrier. Therefore, the foam was injected immediately after excavating the trench. The device during digging the trench and final geometry of the injection body is shown in Fig. 4. The geofoam material for filling the barrier was a PU foam from Uretek Deutschland GmbH that could be injected in the trench without any resistance and expanded freely; all these factors lead to a geofoam with very low density. A laboratory test was carried out for finding the dynamic properties of the geofoam. The results showed a medium density of $0.61kN/m^3$, shear wave velocity of $330m/s$ and poison's ratio close to zero (0.01).

2.3. Test results and discussion

The test results of the field-test are evaluated in terms of the vertical vibration velocities of the soil, which are measured in the time domain and transmitted into the frequency domain by applying Discrete Fourier Transformation (DFT). The results are presented in the frequency domain. An advantage of representing the results in the frequency domain is to visualize the wave interference influences. The final assessment of the effectiveness of the trench is made by comparing the two measurements.

Result of full experimental study for all measured points beyond the geofoam-filled trench are analysed and the results are presented in following figures. In order to ensure reliability of the results, the measurements have been done two times for both before and after installing the barrier.

Fig. 5 shows a significant attenuation for almost all measured points for the frequency between 30 and 60*Hz* by implementing the geofoam-filled trench. The results shows the highest amount of mitigation for the first point after the trench (point C) in comparison with other points. As the frequency of applied load increases, the vertical soil velocity amplitude reduces dramatically and then gradually reaches to a stable value after a frequency of 60*Hz*. The system effectiveness is increased from 37 to 60% by increasing the frequency from 30 to 40*Hz* for point C. A practical comparison can be done between the screening of incident waves for measured points of D and G, where are located at the center and beside of the source in Fig. 3, respectively. The results reveal that we have the highest amount of mitigation in the centreline of the trench in comparison with other areas. The efficiency of the frequency of 40*Hz* for both points D and G are 65 and 35%, respectively, which shows a considerable difference.

However, there is not any attenuation effect for the frequency less than 20*Hz* and it seems that the isolation system is not practical for lower frequencies. Athanasopoulos et al. [34] stated that the attenuation of R-wave amplitude is frequency-dependent and it increases exponentially with the frequency due to both radiation and material damping. Therefore, low frequency of the load results in less attenuation of the propagated waves in the soil. This issue disappears the effectiveness of the trench in mitigating the waves with large R-wavelength (which is equal to low frequency). The same statement can be applied for the reason of not practicability of the trench in high frequencies. Increasing the frequencies result in losing of the wave energy until disappearing. Therefore, there is not any difference between amplitude of the vertical soil particle velocity before and after installing the trench. The results of

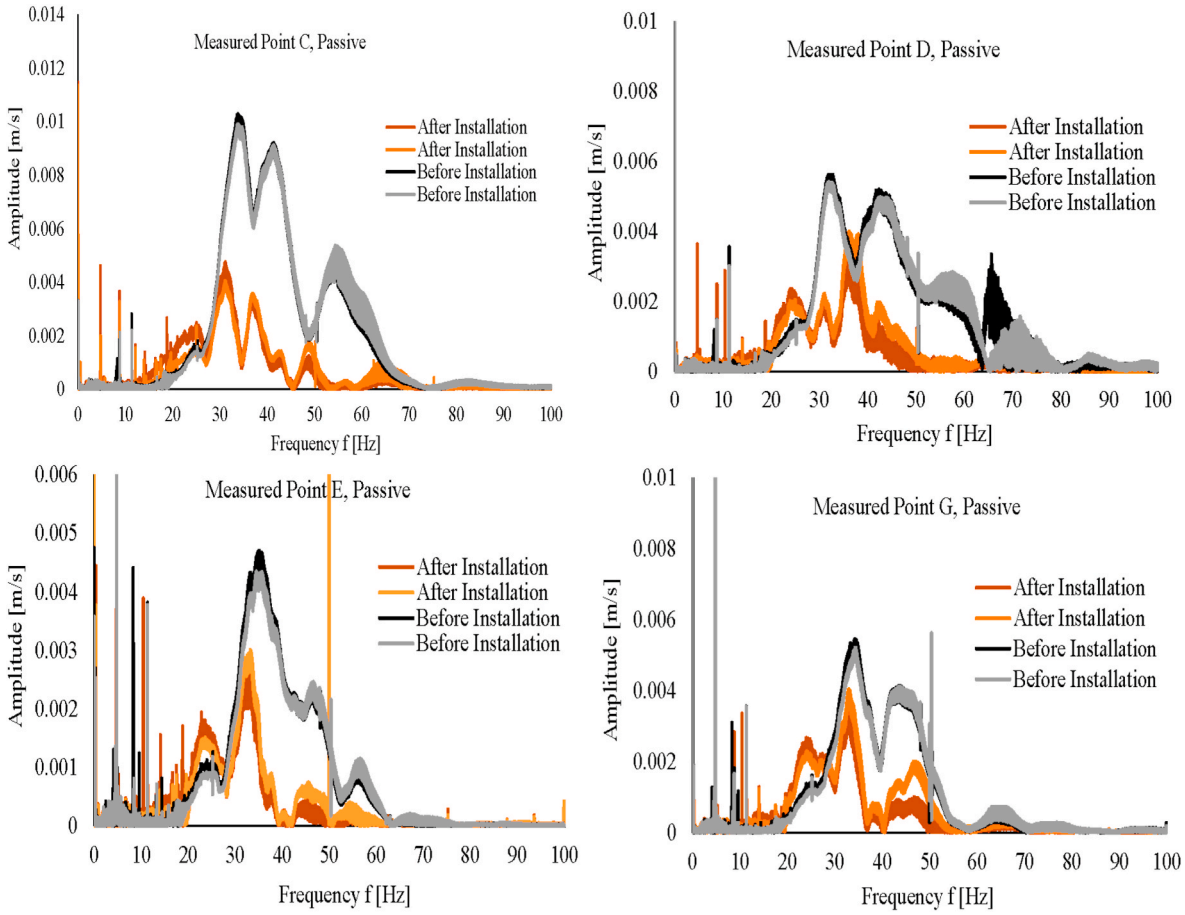

Fig. 6. Representation in the frequency domain: Measuring points C, D, E, G (Passive Isolation).

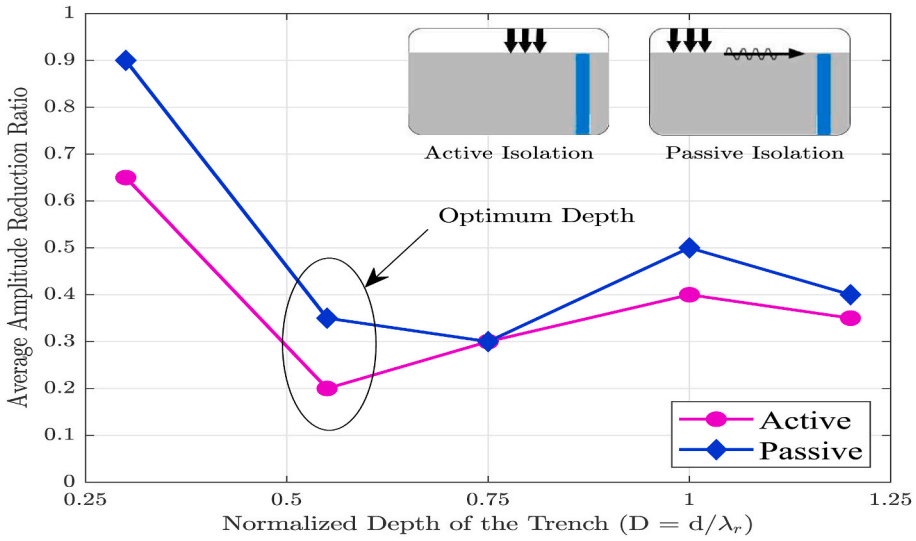

Fig. 7. Influence of normalized barrier depth on $\overline{A}_r$ ($X = 0.5$).

various points for the passive isolation are presented in Fig. 6. The area immediately after the trench has the highest screening performance. The screening performance in attenuation of incident waves increases for the frequency range between 30 to 60*Hz*, whereas this frequency range decreased to $35-50$*Hz* for point E. However, some unexpected peaks and valleys are observed in vertical soil velocity amplitude of 50 and 40*Hz* for points C and D, respectively.

Baidya, et all [35] investigated change of amplitudes of vibrations in layered soil and they stated that many soils in nature exhibit an increase in shear modulus with depth and this issue can be recognized as a reason for distinct peaks and valleys. The incoming waves may reflect and refract at the interfaces of soil layer and they can superpose with surface waves in the same phase and originate a bigger wave, which cause amplification in vertical response of the soil. As it is already mentioned

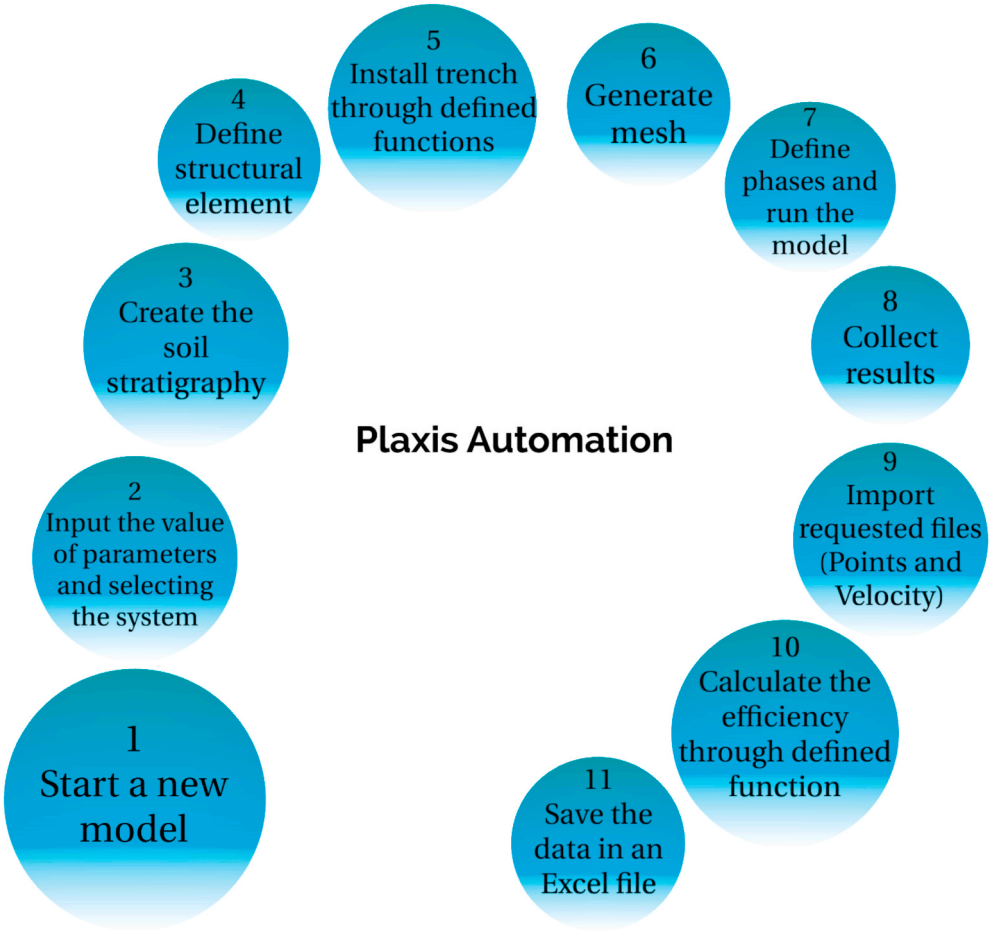
Plaxis Automation
1 Start a new model
2 Input the value of parameters and selecting the system
3 Create the soil stratigraphy
4 Define structural element
5 Install trench through defined functions
6 Generate mesh
7 Define phases and run the model
8 Collect results
9 Import requested files (Points and Velocity)
10 Calculate the efficiency through defined function
11 Save the data in an Excel file

Fig. 8. Automation process of Plaxis model with Python.

in section 2.2, we faced a hard soil during the excavation and for this reason the depth of the trench could not reach the target value ($3.2m$). It means that we have almost a full reflection of incoming waves. Therefore, the unexpected discrepancies in the result can be explained by superposition of surface waves and reflected waves [10]. In addition, Haupt stated that the reflection and refraction of the R-wave energy generates a typical interference pattern, in which the maximum or minimum points usually appear at intervals of half of R-wave [19]. By following the intervals for each minimum/maximum point in the figure, it can be seen that the intervals follow the rules of Haupt. This pattern is generated by the superposition of waves.

Frequency domain analysis of the results enables to monitor normalized trench depth in terms of R-wavelength. Changing the frequency of the load leads to changing the length of R-wave since the shear wave velocity of the soil is constant. Therefore, the effectiveness of the geofoam-filled trench is presented as a normalized depth in Fig. 7.

The results show that increasing D results in decreasing the value of $(\overline{A}_r)$, which means increasing the efficiency of the trench. The lowest value of $(\overline{A}_r)$ is achieved for a normalized depth of approximately 0.6, which agrees with the result of [11].

Average amplitude reduction ratio is expected to decrease with increasing the depth of the trench. However, some amplifications in $(\overline{A}_r)$ are observed after the normalized depth of 0.6. Haupt stated that distinct peak can occur when shear wave velocity of the soil increases proportional with the depth. In addition, Massarsch [4] indicated that refracted waves from the trench and transferred waves beneath the trench can superpose in the same phase and originate a bigger wave, which can cause amplification. Since the soil profile in experimental test is non-homogeneous in terms of increasing shear wave velocity, the unexpected distinct peaks can be explained by superposition of surface waves.

3. Numerical modelling

Since the model is largely affected by the transmitted and reflected waves from the boundary of the model, it is important to keep the region of interest enough far from the reflecting boundary. Therefore, the dimensions of the model are selected as (50, 20, 20 m) and (70, 25 m) in the case of active and passive system, respectively. The soil is modelled as a homogeneous and isotropic half space. The linear elastic model is selected for the soil since the amplitude of generated vibrations are small and the soil does not experience the development of plastic deformations in the region of consideration. In order to applying a special boundary condition, viscous boundaries are applied to the bottom and right sides of the $2D$ and $3D$ models and at Y max direction for $3D$ model, too. A viscous boundary condition, which was introduced by Lysmer and Kuhlmeyer [36] consist of the viscous dampers applied in X, and Y (for $2D$), and Z (for $3D$) direction along the boundary. Relaxation coefficients ($C1$ and $C2$) are introduced in order to improve the effect of absorption. Improving the wave absorption in the normal and tangential direction is done by coefficients $C1$ and $C2$, respectively. The values for both coefficients are selected as 1.

Plaxis uses a global meshing parameter, which is called average element size for showing the quality of the mesh. This parameter is calculated based on the dimensions of the model and the number of elements. The average element size (I_e) of 0.5 is enough for reaching acceptable results and satisfying the criteria of Kuhlemeyer and Lysmer [36] for assuming the average element size less than to one-eight of the

Table 1
Material properties of Proposed FE model.

	γ (kN/m^3)	Poisson's ratio	Shear wave velocity (m/s)	Elastic Modulus (kN/m^2)	Rayleigh damping coefficient (β)
Soil	20	0.3	216	250,000	0.0003183
Geofoam	0.61	0.01	330	13,750	–

wavelength associated to the maximum frequency component of the input wave. The vibration source is modelled as a vertical harmonic load with the amplitude of 1 and frequency of 50*Hz*. The dynamic time interval is considered as 0.5*s*, which is enough to allow the passage of dynamic load. The steel plate under the shaker is modelled as plate and the shaker weight is considered as a uniform distributed load with magnitude of $1kN/m^2$. However, weight of the steel plate and the shaker is kept constant during parametric study since it does not play a significant role in vibration attenuation results and the difference for the efficiency of trench between zero and non-zero foundation weight is 1.5%, which can be neglected [11,33,37].

A large number of models are developed for the parametric study through changing the governing factors of the trench. Creating all models manually is a time-consuming process. In order to save the calculation costs, a script is developed for coupling the finite element model (Plaxis) with Python language. This script allows the user to control both the input and the output of the model via an external Python handler. The main advantage of the automation is accelerating the pace of the parametric study. The input of the script corresponds to the values selected for different parameters, including the depth *D*, width *W*, length *L*, distance between the walls *S* and the location *X*. Three different systems are selected including the single, double and triangle wall for assessing the effect of the shape of the trench on the screening performance. The script starts by creating a borehole and subsequently installs the trench, defines different phases, runs the model and calculates the efficiency of the trench. The entire process is executed automatically as shown in Fig. 8. Different functions are defined for excavating the trench with different configurations including the single, double and the triangular wall. An average amplitude reduction ratio factor ($\overline{A}_r$) is used for finding the efficiency of the trench beyond the trench. The value of ($\overline{A}_r$) is the average value of vertical soil velocity before and after the installation of the trench. Finally, the data for each system are stored in an Excel file. The created Python script for 2*D* and 3*D* model are provided in the Appendix.

The soil properties for the following analysis are considered the same as those measured in the field test, which are presented in Table 1. The constant frequency of $f = 50Hz$ is selected for the applied load, which results in R-wavelength equal to 4*m*. In addition, the linear elastic behaviour is used for both the geofoam and soil in the further calculations. The parameters α and β are Rayleigh coefficients that determine the effect of mass and stiffness in the damping of system, respectively. In mass proportional damping, damping forces are generated by velocities of the model and simulated the model's movement through a still viscous fluid. Therefore, motion at points within the model cause damping. It should also be observed that the mass proportional damping would give damping due to rigid body motions. In stiffness proportional damping, damping is generated by strain rates. Therefore, the damping is more related to the material in comparison with motion of the model. Hence, stiffness proportional damping is used in this finite element model [14]. In addition, in many practical soil related problems, α is ignored since it can lead to undesirable result if a large mass has been introduced into the model [38–40].

3.1. Experimental validation of finite element method

The developed model has been validated using the results of the field test for the active and passive isolations. The measured and the calculated wave attenuation curves are depicted in Figs. 9 and 10 using a logarithmic scale for different excitation frequency including, 20, 35, 50 and 65*Hz*, respectively.

The FEM results are in line with the trends in the experimental results and there is a reasonable agreement between the normalized vertical soil particle velocities, obtained for both the active and passive cases. Nonetheless, unexpected valleys are visible in the results. Propagated waves through and underneath the geofoam-filled trench are sometimes in or out of phase. This results in a destructive interference of waves and creates valleys in numerical modelling results [21].

Another reason of observing some irregular peaks in the results is the less normalized distance between the points for presenting the numerical modelling, which is 0.25. This distance results in presenting the

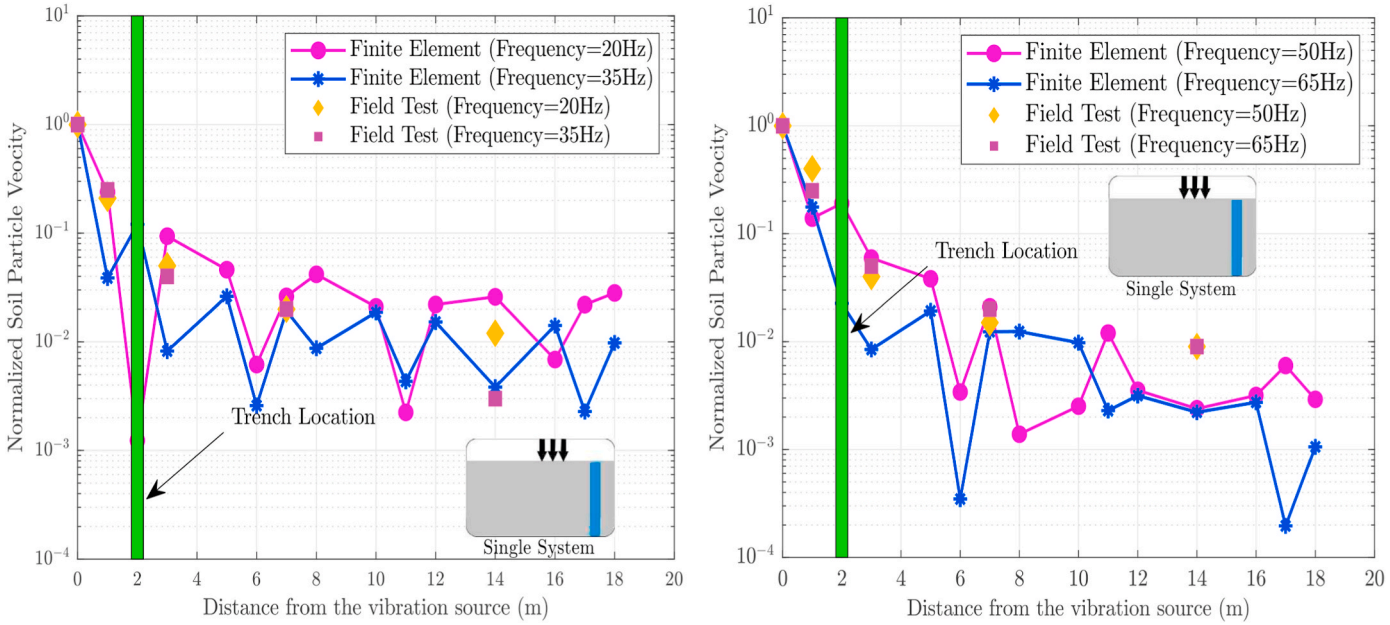

Fig. 9. Validation of numerical modelling based on the result of field test, active isolation, (D = 3 m, W = 0.25 m, L = 10 m, X = 2 m).

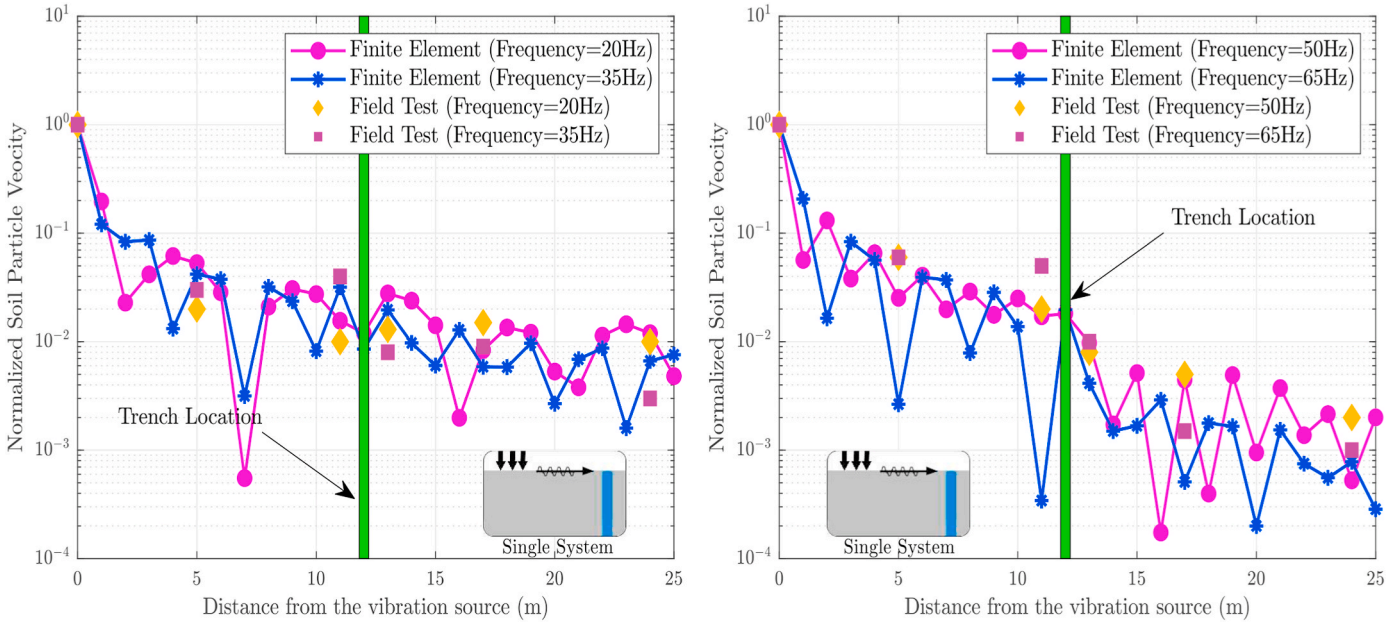

Fig. 10. Validation of numerical modelling based on the result of field test, passive isolation (D = 3 m, W = 0.25 m, L = 10 m, X = 12 m).

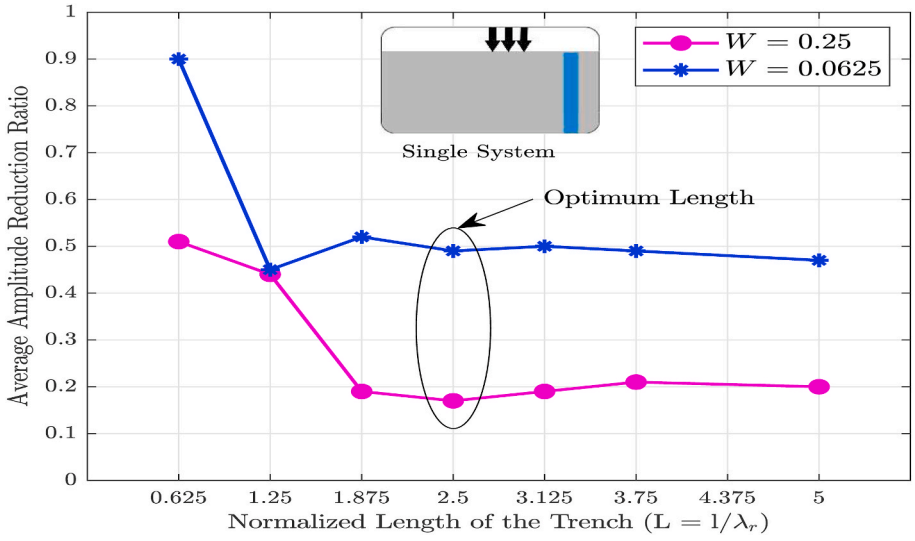

Fig. 11. Influence of normalized barrier length on $\overline{A}_r$ ($X = 1.25$, $D = 1.25$).

results as detailed as possible and showing all irregularities that may happen for the area after the trench. The same figure has been illustrated with normalized distance of 0.5 and fewer irregularities have been observed with new distance but the results of this distance is not presented here Therefore, the model developed in this study, including the wave absorbing boundary, adequately predicts the vibration propagation problem for the case of the geofoam-filled trench.

4. Active isolation

A comprehensive parametric investigation is carried out to evaluate the effectiveness of different isolation systems including the single, double and triangular walls as the wave barriers for the active isolation due to the harmonic load in the vertical direction. Results of the detailed parametric investigation are presented and some applicable recommendations are suggested for designing the wave barriers.

The parametric study begins with considering the different normalized values with respect to the R-wavelength for parameters of the trench including the depth D (from 0.5 to 2.5), the width W (from 0.0625 to 0.25) and the length L (from 0.625 to 5), respectively. All parameters are normalized with respect to the R-wavelength. The different geometrical parameters are considered to be the same for all configurations in this paper. Three different normalized locations including 0.5, 1.25 and 2 are selected for computing the efficiency of the geofoam-filled trench. Since the efficiency of the barrier for all three systems is not affected by the location of the trench, the result of one location (0.5) is presented.

4.1. Single wall system

The normalized soil particle velocity before and after installing the trench was compared for an area beyond trench. The geofoam-filled trench was installed at the normalized location of 0.5. The results, which are not presented here showed that there is not any considerable difference after distance of $7.5\lambda_r$ for both with and without trench for the area beyond the barrier. This leads to use $7\lambda_r$ for the screened zone for

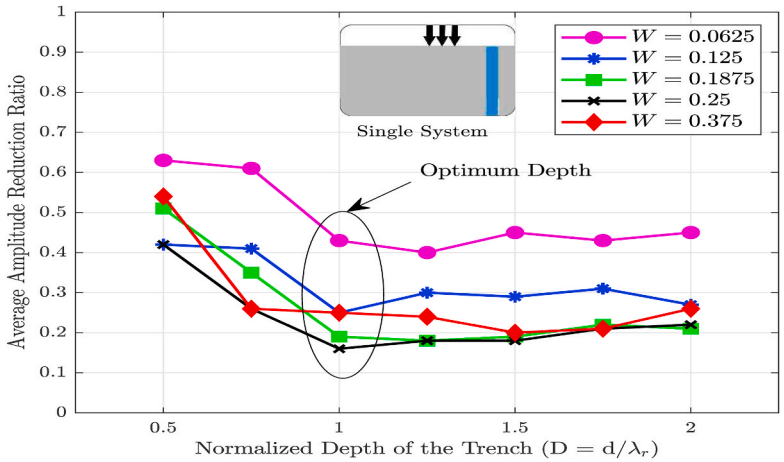

Fig. 12. Influence of normalized barrier depth on $\overline{A}_r(X = 0.5)$.

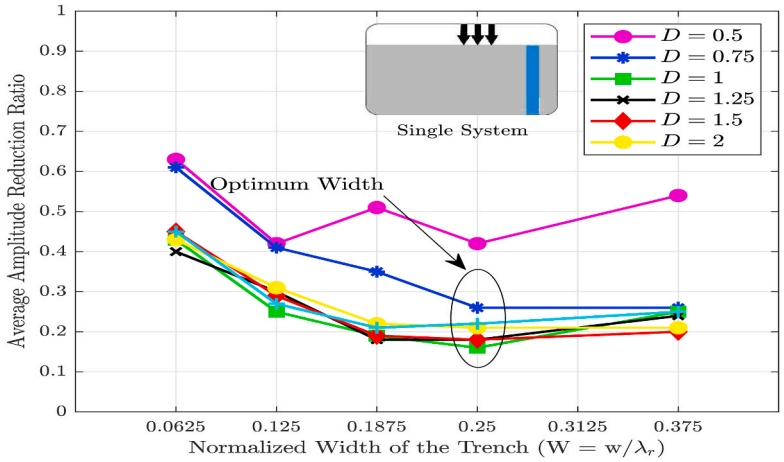

Fig. 13. Influence of normalized barrier width on $\overline{A}_r$ $(X = 0.5)$.

calculating $\overline{A}_r$. This value is selected for all systems in the active scheme.

4.1.1. *Effect of trench dimensions*

Fig. 11 shows that $\overline{A}_r$ decreases dramatically, which is the result of increasing the normalized length from 0.625 to approximately 2.5. It is apparent from the figure that the normalized length beyond around 2.5 does not create any changes and may be conservatively assumed to remind unchanged thereafter. The same parametric study has been applied to other systems with the same results. Therefore, the normalized length of the trench is considered as 2.5 for other systems as well.

The influence of varying the depth of the EPS Geofoam wave barrier is studied and the results are presented in Fig. 12.

We achieve a considerable amount of wave attenuation by increasing the depth of the barrier from 0.5 to 1 for all widths. A gradual increase or

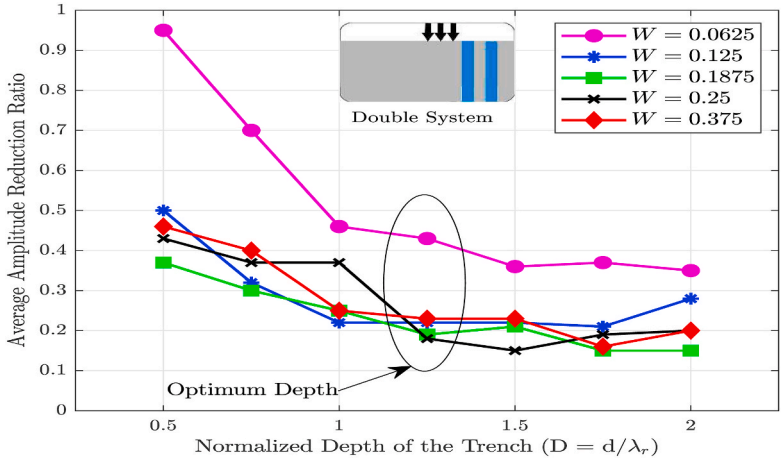

Fig. 14. Influence of normalized barrier depth on $\overline{A}_r$ $(X = 0.5)$.

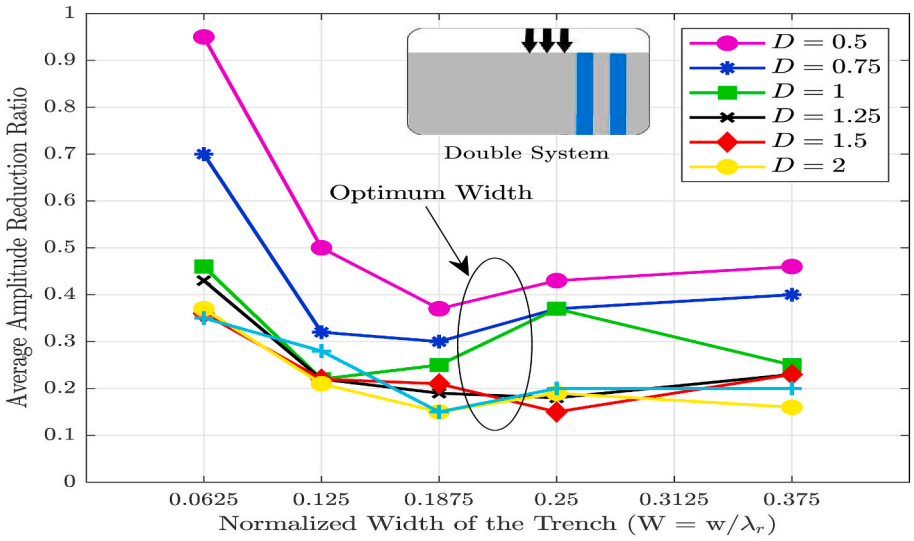

Fig. 15. Influence of normalized barrier width on $\overline{A}_r$ ($X = 0.5$).

decrease in wave attenuation is observed when increasing the normalized depth up to 1. It is observable that there are not significant discrepancies after this depth. Hence, the depth of 1 is defined as the optimum depth for all widths for blocking a major portion of incoming waves. The optimum D has a direct relationship with the width of the barrier.

Fig. 13 shows that W plays a significant role in screening efficiency of the geofoam-filled obstacle. It is apparent that in general the wave attenuation reaches its maximum amount at a W value around 0.25. For wider trenches ($W > 0.2$), the effect of W is negligible and can be ignored. Increasing the width of the barrier means having more distance between the two sides of the obstacles, which is leading to additional geometric discontinuities in the boundary area and results in a further refraction phenomena of the incoming R-waves.

4.2. Double wall system

Attenuation of incident waves through a double wall system may be advantageous in circumstances where the implementation of a single wall system is difficult because of unrealistic depth. Using a pair of geofoam-filled barriers may possibly require lower depth in comparison with the single wall system. The efficiency of the double wall system is compared to a single wall with a thickness of $2W$, having the same width, depth and length as the single wall obstacle. Therefore, the width of both walls are considered as one width, which is the normalized width W for both trenches. At the first step, a parametric study is investigated for finding the optimum spacing between the barriers to achieve the best performance. A parametric study has been done to find the optimum space between the wall and the normalized space of 0.5 is selected for this parametric study. However, the result of the parametric study is not presented in this paper. This space is verified with the results of [31] for optimum distance between trenches.

4.2.1. Effect of trench dimensions

The information of Fig. 14 shows that D governs the wave screening for the normalized depth between 0.5 and 1.25 for all widths. The optimum depth of almost 1.25 is selected for all barriers. The results show that D plays a more significant role for narrow trenches than for wider trenches.

At the corners of the trench, mode conversion, that is converting R-wave to body wave occur, due to passing the incoming waves through the edges of the obstacle into the region behind this. Since the diffraction

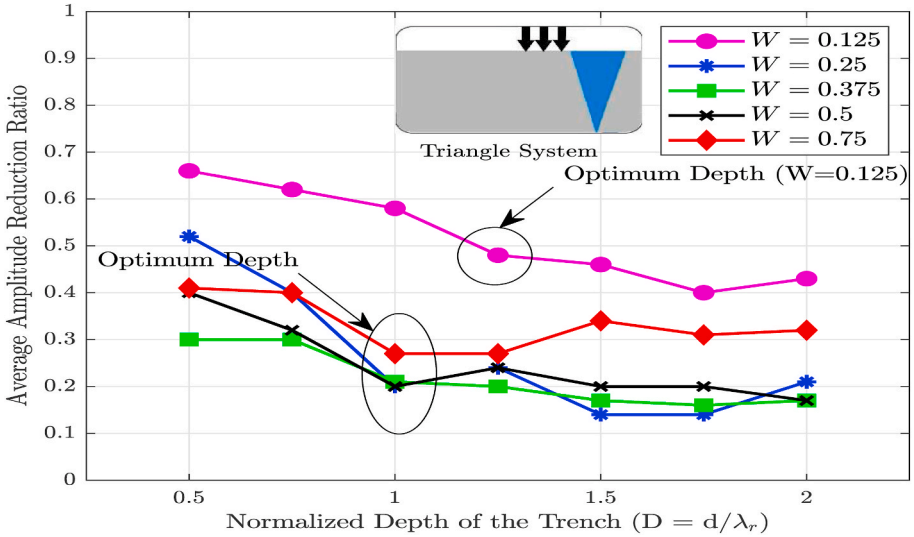

Fig. 16. Influence of normalized barrier depth on $\overline{A}_r$ ($X = 0.5$).

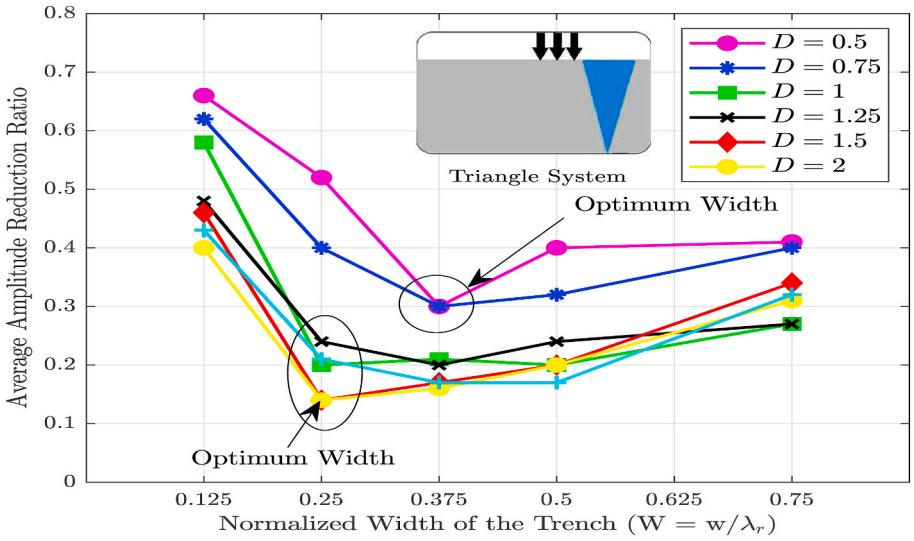

Fig. 17. Influence of normalized barrier width on $\overline{A}_r$ of EPS Geofoam wave barrier ($X = 0.5$).

effect is low for a narrow trench ($W = 0.0625$), due to the shorter distance between the two corners of an obstacle, the effect of D is more visible. For wider trenches ($W > 0.0625$), the influence of the diffraction phenomenon is greater than the effect of D. All of these issues indicate that the diffraction phenomenon plays an important role in the wave attenuation process for the double wall system.

As seen in Fig. 15, $\overline{A}_r$ decreases dramatically by increasing the normalized width of the trench from 0.0625 to around 0.2. Thereafter, it remains at a constant value while W reaches to 0.375. An optimum width of almost 0.2 is selected for achieving the efficiency of approximately 70% and 80%. In addition, the influence of W is lower for barriers with D higher than 0.75 and the graphs of deeper trenches follow lower slopes for reaching the optimum width (0.2) from the start point ($W = 0.0625$).

According to developed theory by Ref. [41], the energy of R-wave in a region between the ground surface and the R-wavelength (at normalized depth of the trench) is partially reflected at the zone of wave shadow. The R-wave energy passing beneath the obstacle creates a new R-wave at some distance beyond the barrier. The energy of the passing R-wave creates vibrations in the crucial zone. Increasing the width of the trench blocks more incoming waves and lead to passage fewer incident waves.

4.3. Triangular wall system

A large part of the energy of a dispatched wave is in the form of R-wave. In addition, the amount of transferred energy by incident waves from an interface to the screened zone is a function of the incident angle. The ratio of the reflected to transferred R-wave energy is a function of the corner angle of the trench. The angle of the barrier wall and the ground surface is recognized as one of the most important factors in distributing energy among the waves. Moreover, as discussed in the previous sections for the single and double wall systems, the normalized width of the barrier appears to be one of the most important parameters that will govern the screening effectiveness of the trench. We achieve more wave attenuation by increasing the width of the trench even in the case of shallow trenches. For a proper comparison between all configurations, the triangular system is considered with the same depth and the same cross-sectional area as the single and double wall trench; however, the width of its trench is different from that of the other two systems.

4.3.1. Effect of trench dimensions

As shown in Fig. 16, increasing the normalized depth of the trench from 0.5 to almost 1.25 for the narrow trench leads to an increase in the efficiency of the trench. However, if the width of the trench increases ($W > 0.25$), a smaller decrease in $\overline{A}_r$ is visible in comparison with narrow trenches. A normalized depth of 1 and 1.25 is considered for optimum depth to achieve an acceptable amount of wave attenuation for narrow and wider trenches, respectively.

Fig. 17 shows the influence of W on screening performance. A wider trench is sufficient (for $D < 0.75$) for reaching an acceptable level of screening performance (around 75%), while by increasing the normalized depth of the trench ($D > 0.75$), a slender barrier is needed for the effective trench ($W = 0.25$).

Increasing the depth of the trench means hindering more incoming waves. For the shallow trench, as the corner of the barrier is near to the ground surface, the role of mode conversion of R-waves into body waves becomes apparent. However, in the case of deeper trenches, the corner of the trench move further into the soil. Therefore, the effect of the diffraction, which is resulting of passing the wave around a trench edge (trench corner) becomes smaller. Thus, a slender obstacle is needed to achieve an admissible amount of vibration for deep trenches.

5. Passive isolation

A 2D time domain finite element model is established for presenting the result of the parametric investigation. Increasing the normalized distance between the obstacle and vibration source can lead to making R-waves more prevailing in comparison with body waves [3,18]. If the barrier encounters plane waves, a plane strain model can present reliable results for calculating average amplitude reduction ratio. Another reason is saving the computational time. Since the geometry of passive is bigger than active model, analysing several models would require a lot of time. In addition, several researches [11,26] showed that the result of 2D and 3D models are in acceptable agreement. Different parameters including trench depth, width and location are considered for studying the effectiveness of the trench.

5.1. Single wall barrier

The variation of the barrier's dimensional factors (including depth and width) is determined in the same way as in the active isolation scheme. However, the geometric factor (including distance between the obstacle and vibration source) is determined to be 3. The reduction zone

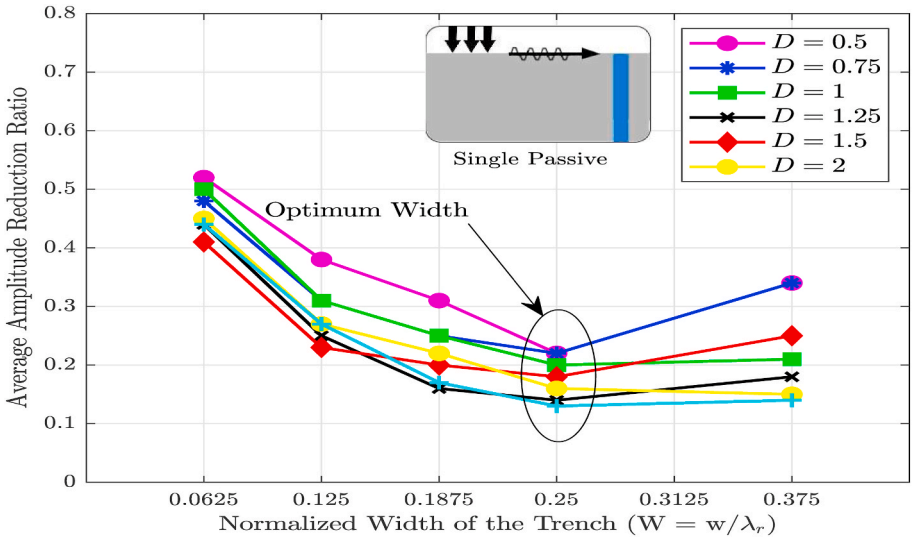

Fig. 18. Influence of normalized barrier width on $\overline{A}_r$ ($X = 3$).

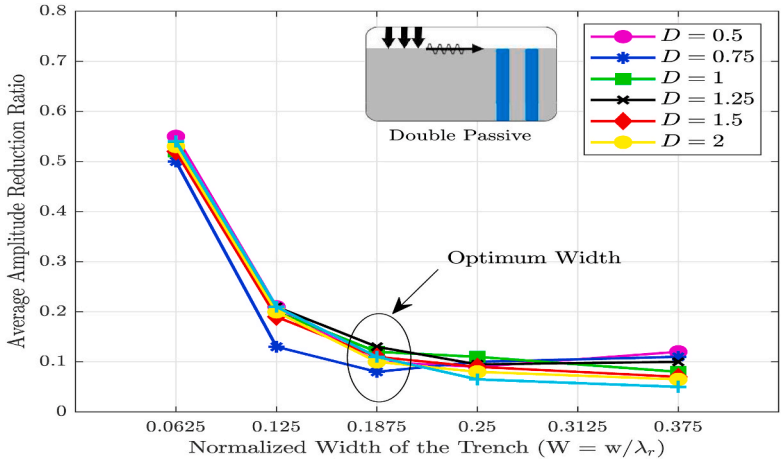

Fig. 19. Influence of normalized barrier width on $\overline{A}_r$ ($X = 3$).

study of the single wall trench, which is not presented in detail, showed a considerable reduction in vertical ground displacement before and after installing the geofoam-filled trench for a normalized distance of 10, which is selected for calculating $\overline{A}_r$.

5.1.1. Geometric factor study

The result of $\overline{A}_r$ as a function of W is plotted in Fig. 18. A careful study of this figure reveals that there is no substantial relationship between the computed $\overline{A}_r$ value and the normalized depth.

On the other hand, increasing the wall thickness leads to further scattering of the ground vibrations generated by source of disturbance. A reduction of approximately 60% is achieved by increasing W from 0.0625 to 0.25 for almost all trench depths and it seems that $W = 0.25$ is the optimum width for achieving a reasonable amount of wave attenuation. An increase in trench thickness creates more discontinuity at the ground surface with different dynamic properties and this difference creates a diffraction in incident waves.

5.2. Double wall barrier

Fig. 19 shows that $\overline{A}_r$ is not affected by the trench depth and even increasing W cannot create any change in the influence of D on $\overline{A}_r$. Some of the incident R-waves reflect downward to the left of the obstacle after encountering the left side of first wall and the remaining one transmit to the right of the barrier. Subsequently, the transmitted R-waves reflect again through the discontinuity at the second wall. In fact, the diffraction and mode conversation due to the corners of a pair of trenches play more significant role in decaying the incoming R-waves in comparison with the depth, and this issue outweighs the role of trench depth.

Wider barriers lead to better screening effect and W seems to govern the screening process. For the narrow trench however, increasing the normalized width ($W > 0.2$) results in decreasing the effect of W, owning the fact that increasing the width of the barriers hardly affects the screening vibration at any depth. Since the thickness of the obstacle reaches a certain value, increasing width of the barrier hardly affect the screening vibration for almost all depths. Increasing the normalized width leads to more discontinuity in the ground surface with different shear modulus hindering more ground-born vibration. However, since W continuously increases, the probability of having wave interferences among the R-waves that are propagated through the trench and the waves that are transmitted beneath the obstacle due to different velocity. This phenomenon may be one of the reasons for reaching to a stable value of the normalized width beyond 0.25.

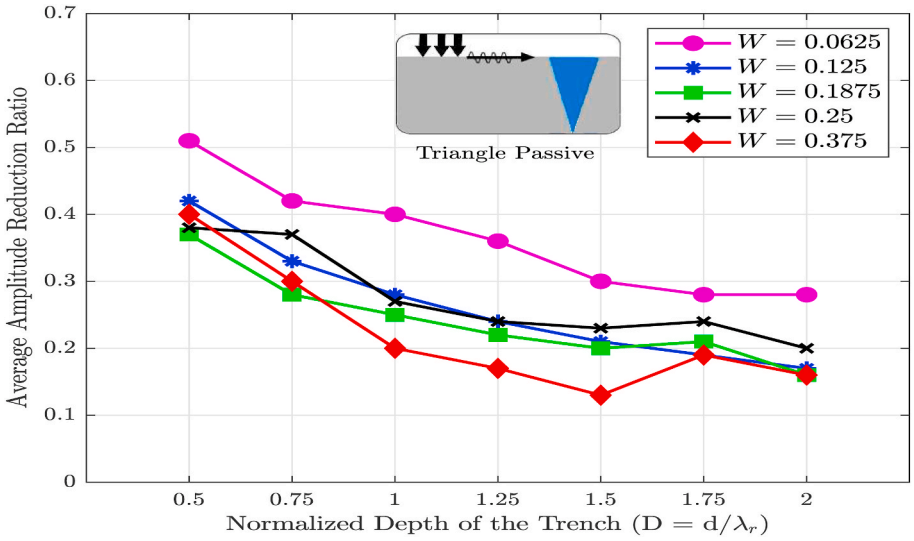

Fig. 20. Influence of normalized barrier depth on $\overline{A}_r$ ($X = 3$).

5.3. Triangular wall barrier

As it can be seen in Fig. 20, the efficiency of the trench increases gradually and continuously by increasing the normalized depth for approximately all widths, implying that D governs the scattering influence. It is apparent from the figure that the barrier width has an ignorable influence on the scattering of incoming energy. Considering the corner of the triangular wall barrier, its shape can be the reason for observing no mode conversion or diffraction phenomenon that changes the R-waves to body waves.

6. Conclusion

Based on a fully experimental test, a comprehensive numerical modelling for evaluating the efficiency of the geofoam-filled barrier in attenuating dispatched waves has been performed. The conclusions drawn from field work and parametric studies can be summarized as follows:

Active isolation can be a better solution for hindering of incident waves in comparison with the passive isolation based on the results of field test. However, the results also showed that the first point after the trench has the highest amount of mitigation and normalized depth of $0.6\lambda_r$ is enough for reaching the highest value of the efficiency for both active and passive isolation systems.

The parametric study of the active and passive isolations showed the zone of $7\lambda_r$ and $10\lambda_r$ as crucial zones for an area after the trench for computing $\overline{A}_r$. This finding proves that the vibration isolation system should be divided into active and passive systems during analysing.

Analysing the result of the active scheme demonstrated that the optimum length can be considered as $2.5\lambda_r$ for all three systems for reaching the highest value of the efficiency. The depths of $1\lambda_r$, $1.2\lambda_r$ and $1\lambda_r$ are considered as the optimum depths for the single, double and triangular wall systems, respectively. Concerning the effect of width of the geofoam-filled trench, it is concluded that the value of $W = 0.2$,0.2 and 0.25 are enough for considering the optimum W for single, double and triangular wall systems, respectively.

On the other hand, evaluation of the passive isolation revealed that the depth of the barrier hardly affects the efficiency of the obstacle for single and double wall systems and the influence of D can be ignored as long as $D > 0.5$. While, D is a key factor in scattering of incoming waves for the triangular wall system. However, an optimum depth cannot be selected for this system as the efficiency of the obstacle increases gradually and continuously by increasing D. The normalized width has to be increased to approximately 0.25 to have a successful single wall system. For the double wall system, W should be at least 0.2 for having satisfactory influence of screening. The barrier's width has a negligible effect on the scattering of dispatched waves for the triangular wall system. In addition, the parametric study of the trench location for both active and passive schemes demonstrated that this factor is not an important parameter that influences the efficiency of the geofoam-filled trench.

Declaration of competing interest

The authors declare that they have no known competing financial interests or personal relationships that could have appeared to influence the work reported in this paper.

References

[1] Miller GF, Pursey H, Crisp Bullard Edward. On the partition of energy between elastic waves in a semi-infinite solid. Proc Roy Soc Lond Math Phys Sci 1955;233 (1192):55–69.
[2] Richart Frank Edwin, Hall John Russell, Woods Richard D. Vibrations of soils and foundations. 1970.
[3] Al-Hussaini Tahmeed Malik. Vibration isolation by wave barriers. 1993.
[4] MASSARSCH KR. Vibration isolation using gas-filled cushions, soil dynamics symposium to honor prof. richard d. woods. Austin, Texas: Geofrontiers; 2005. January 24-26, 2005.
[5] Mahdavisefat E, Salehzadeh H, Heshmati AA. Full-scale experimental study on screening effectiveness of srm-filled trench barriers. Geotechnique 2018;68(10): 869–82.
[6] Coulier Pieter, Cuéllar Vicente, Degrande Geert, Lombaert Geert. Experimental and numerical evaluation of the effectiveness of a stiff wave barrier in the soil. Soil Dynam Earthq Eng 2015;77:238–53.
[7] Gao Guangyun, Zhang Qiwei, Chen Juan, Chen Qingsheng. Field experiments and numerical analysis on the ground vibration isolation of wave impeding block under horizontal and rocking coupled excitations. Soil Dynam Earthq Eng 2018;115: 507–12.
[8] Bose Tulika, Choudhury Deepankar, Sprengel Julian, Ziegler Martin. Efficiency of open and infill trenches in mitigating ground-borne vibrations. J Geotech Geoenviron Eng 2018;144(8):04018048.
[9] Woods Richard D. Screening of suface waves in soils. 1968.
[10] Ulgen D, Toygar O. Screening effectiveness of open and in-filled wave barriers: a full-scale experimental study. Construct Build Mater 2015;86:12–20.
[11] Alzawi Ashref, El Naggar M Hesham. Full scale experimental study on vibration scattering using open and in-filled (geofoam) wave barriers. Soil Dynam Earthq Eng 2011;31(3):306–17.
[12] Pu Xingbo, Shi Zhifei, Xiang Hongjun. Feasibility of ambient vibration screening by periodic geofoam-filled trenches. Soil Dynam Earthq Eng 2018;104:228–35.
[13] Çelebi Erkan, Fırat Seyhan, Beyhan Günay, Çankaya İlyas, Vural İsa, Kırtel Osman. Field experiments on wave propagation and vibration isolation by using wave barriers. Soil Dynam Earthq Eng 2009;29(5):824–33.
[14] Murillo Carol, Thorel Luc, Caicedo B. Ground vibration isolation with geofoam barriers: centrifuge modeling. Geotext Geomembranes 2009;27(6):423–34.

[15] Beskos DE, Dasgupta B, Vardoulakis IG. Vibration isolation using open or filled trenches. Comput Mech 1986;1(1):43–63.
[16] Leung KL, Beskos DE, Vardoulakis IG. Vibration isolation using open or filled trenches. Comput Mech 1990;7(2):137–48.
[17] Beskos Dimitri E. Boundary element methods in dynamic analysis: Part ii (1986-1996). Appl Mech Rev 1997;50(3):149–97.
[18] Ahmad S, Al-Hussaini TM. Simplified design for vibration screening by open and in-filled trenches. J Geotech Eng 1991;117(1):67–88.
[19] Haupt WA. Wave propagation in the ground and isolation measures. 1995.
[20] Haupt WA. Isolation of vibrations by concrete core walls. In: Proceedings of the ninth international conference on soil mechanics and foundation engineering, vol. 2; 1977. p. 251–6.
[21] Ekanayake Sanka D, Liyanapathirana DS, Jian Leo Chin. Attenuation of ground vibrations using in-filled wave barriers. Soil Dynam Earthq Eng 2014;67:290–300.
[22] Liyanapathirana DS, Ekanayake Sanka D. Application of eps geofoam in attenuating ground vibrations during vibratory pile driving. Geotext Geomembranes 2016;44(1):59–69.
[23] Majumder Mainak, Ghosh Priyanka, Rajesh S. An innovative vibration barrier by intermittent geofoam-a numerical study. Geomech. Eng. 2017;13(2):269–84.
[24] Majumder Mainak, Ghosh Priyanka, Rajesh S. Numerical study on intermittent geofoam in-filled trench as vibration barrier considering soil non-linearity and circular dynamic source. Int J Geotech Eng 2017;11(3):278–88.
[25] Majumder Mainak, Ghosh Priyanka. Intermittent geofoam in-filled trench for vibration screening considering soil non-linearity. KSCE J. Civ. Eng. 2016;20(6):2308–18.
[26] Qiu Bo, Ali Limam, Djeran-Maigre Irini. Numerical study of wave barrier and its optimization design. Finite Elem Anal Des 2014;84:1–13.
[27] Saikia Ankurjyoti. Numerical study on screening of surface waves using a pair of softer backfilled trenches. Soil Dynam Earthq Eng 2014;65:206–13.
[28] Schevenels M, Lombaert G, et al. Double wall barriers for the reduction of ground vibration transmission. Soil Dynam Earthq Eng 2017;97(1–13).
[29] Esmaeili Morteza, Ali Zakeri Jabbar, Ali Mosayebi Seyed. Investigating the optimized open v-shaped trench performance in reduction of train-induced ground vibrations. Int J GeoMech 2013;14(3):04014004.
[30] Zakeri Jabbar-Ali, Esmaeili Morteza, Mosayebi Seyed-Ali. Numerical investigation of the effectiveness of a step-shaped trench in reducing train-induced vibrations. Proc Inst Mech Eng - Part F J Rail Rapid Transit 2014;228(3):298–306.
[31] Ph DP Eng Alzawi Ashref, El Naggar M Hesham. Numerical investigations on vibration screening by in-filled geofoam trenches. In: 64rd Canadian geotechnical conference, Toronto, ON, Canada; 2011. ,(Accepted).
[32] Sprengel Julian. Optimierung der praktischen Anwendbarkeit aufgeschäumter Isolierkörper im Boden zur Erschütterungsreduktion. PhD thesis. RWTH Aachen University; 2017.
[33] Saikia Ankurjyoti. Numerical investigation on vibration isolation by softer in-filled trench barriers. J Geo Eng Sci 2016;3(1):31–42.
[34] Athanasopoulos GA, Pelekis PC, Anagnostopoulos GA. Effect of soil stiffness in the attenuation of Rayleigh-wave motions from field measurements. Soil Dynam Earthq Eng 2000;19(4):277–88.
[35] Baidya DK, Murali Krishna G. Investigation of resonant frequency and amplitude of vibrating footing resting on a layered soil system. Geotech Test J 2001;24(4):409–17.
[36] Kuhlemeyer Roger L, Lysmer John. Finite element method accuracy for wave propagation problems. J Soil Mech Found Div 1973;99. Tech Rpt.
[37] Kattis SE, Polyzos D, de Beskos. Modelling of pile wave barriers by effective trenches and their screening effectiveness. Soil Dynam Earthq Eng 1999;18(1):1–10.
[38] Izzat Muhammad Idriss and Harry Bolton Seed. The response of earth banks during earthquakes. Technical report; 1966.
[39] Iodice M, Rustighi E, Muggleton J. Comparison of soil excitation methods for surface wave speed measurements. 2014.
[40] Wilson Edward L. Three-dimensional static and dynamic analysis of structures. 2002.
[41] Dolling Hans-Joachim. Abschirming von erschütterungen durch bodenschlitze. Bautechnik 1970;5:151–8.
[42] Mistler Dr-Ing Michael, Heiland Prof Dr-Ing Dieter. Mobiler Shaker für die künstliche Ersatzanregung bei baudynamischen Fragestellungen, Messtechnik im Bauwesen. Ernst & Sohn Special; 2014.